Available online at www.pelagiaresearchlibrary.com

Pelagia Research Library

Advances in Applied Science Research, 2011, 2 (2): 38-47

Pelagia Research Library
ISSN: 0976-8610
CODEN (USA): AASRFC

Structure Visualization and Surface Microstructural Investigations on Ni-Ti-O Mixed Oxide with ABX_3-Structure of Casted Ni-Superalloy

Khaled M. Elsabawy[a,c,*] and Nader H. Elbagoury[b,c]

[a]*Materials Science Unit-Chemistry Department, Faculty of Science, Tanta University, Tanta, Egypt*
[b]*Casting Technology Lab., Manufacturing Department, Central Metallurgical Research and Development Institute (CMRDI), Helwan, Cairo, Egypt*
[c]*Chemistry Department, Faculty of Science, Taif University, Alhawyah, Taif City, Saudi Arabia*

ABSTRACT

Ni-based super-alloy was synthesized by using conventional casting technique under vacuum and highly superheated treatment route . 3D-microstructural imaging map of the Ni-based super-alloy was constructed depending upon AFM-data evaluating that the morphology of the alloy-surface is a function of composition and preparation conditions .Furthermore raman spectra of casted Ni-based super-alloy was performed to confirm existence of different phases recorded via SEM and EDX-elemental analysis with their corresponding different vibrational modes such as Ni-O vibrating modes in the region 360-510 cm^{-1} and Ti-O vibrating mode which lie at 451,701 and 920 cm^{-1} respectively . A visualized study was made to prove existence of Ni-Ti-O mixed oxides with the ABX_3 structure type .

Keywords: Synthesis; Casting; Raman Spectra; SEM; AFM; 3D-microstructre.

INTRODUCTION

Nickel-based superalloy possess excellent corrosion and oxidation resistance in addition to high strength and ductility at high temperature, ranging from 873 to 1673 K. Strengthening is attributed to the precipitation of the ordered $L1_2$ γ′-phase within the f.c.c. γ-phase. The precipitates composition is $(Ni,X)_3(Al,Y)$, in which Ni-like elements (X) are Cr and Fe and Al-like elements (Y) are Ti and Nb [1].

Although precipitation in these alloys has been studied using sophisticated experimental techniques [2], [3], [4], [5] and [6], information about the early stages of decomposition,

involving nucleation and growth of precipitates is still insufficient and, therefore, the physical mechanisms of these processes are not completely understood [7].

Positron annihilation lifetime spectroscopy (PALS) is sensitive to vacancy-like defects in solids. In comparison with imaging and diffraction techniques, it has the advantage of being non-destructive. A recent review [8] reports on the progress of the application of positron annihilation spectroscopy (PAS) techniques to the study alloy decomposition. Only a few papers report PAS studies on precipitation in Ni-based superalloy ([9] and [10] and references therein).

One of the key points of numerous studies dealing with the precipitation of the γ′-phase is to ascertain whether ordering and clustering occur simultaneously or not, and whether transformations are continuous or follow a nucleation-and-growth process. Theoretical models based on free-energy diagrams, depending on composition and order parameters, describe the different possible paths of the decomposition [11] and [12].

Other studies also reported the occurrence of η phase at the periphery of the γ / γ’ eutectics [13-15].

Many researchers through laser raman spectroscopy (LRS) investigations suggest that probability of existing species like oxides, hydroxides, oxy hydroxides, nitrates, nitrides, sulphates, chlorides and oxy chlorides of Fe ,Cr and Ni could be present in the passive film and surface layers of synthesized M-based-alloy [16-25] . The contributions of other elements apart from Ti ,W, Al, Mo and Co, were not expected to be detected in surface layer, since their content in the alloy was very low to be detectable.

The major goal of the present article firstly is to investigate the micro-structural parameters of different phases existed (even those with low content as Ni-Ti-X_3 where X = Oxygen) on the alloy surface and their vibrational modes detectable thoroughly raman spectroscopic analysis and secondly visualization of $NiTiO_3$-structure type to confirm its presence in the interfacial layers of nickel alloy .

MATERIALS AND METHODS

II. Experimental

The Ni-based alloy used in this work was received as turbine blade scrap supplied from a gas turbine power plant. Table 1 shows the chemical composition of as-received alloy. This scrap was double melted and cast under vacuum using an induction vacuum furnace. In the second melt some amounts of alloying elements such as Ti, Co, Ta, W were added to adopt the chemical composition, then a third melting was made to ensure melting and homogenous distribution of all alloying elements in the heat. Heats were made by melting 10 kg of turbine blade scrap. Pouring was carried out into an investment casting ceramic mold.

The chemical composition of the prepared experimental polycrystalline Ni base superalloy is shown in Table 1. Optical emission apparatus, ARL3560OES as well as Ni base software were used to determine the chemical composition of as-cast alloys.

The X-ray diffraction (XRD) measurement was carried out at room temperature on the ground samples using Cu-K_α radiation source and a computerized Shimadzu (Japan) diffractometer with two theta scan technique.

Table 1. Chemical composition of as cast Ni base superalloys

Elements / Alloy	C	Cr	Mo	W	Ti	Co	Al	Nb	Ta	Ni
Ni-Based-Alloy	0.13	15.01	1.97	2.81	3.63	7.67	4.52	1.07	1.27	Bal.
As cast (H)	0.54	16.95	2.45	4.36	5.88	10.48	1.49	0.10	1.86	Bal.

The microstructure of as-cast specimens was investigated JOEL JSM-5410 Scanning Electron Microscope (SEM). The specimens for microstructure examination were cut from the cast ingots then ground, polished and etched with 100ml H_2O + 50ml HCL + 50ml H_2SO_4 + 4g $CuSO_4$ solution. Studying the microanalysis and segregation for alloying elements was performed using EDS in JEOL JSM5410. Samples were scanned on Analytical Scanning Electron Microscopy for the Jeol JSM-63OLA and VEECO INNOVA -AFM with multi-modes function USA. Raman laser of samples were measured on the Bruker FT Raman with laser source 50 mW.

RESULTS AND DISCUSSION

Structural and Microstructural Measurements (XRD/3D-AFM) :

Fig.1_a show the theoretical XRD-pattern of Ni-Ti-oxide with ABX_3 structure type that compared with actual XRD-profile supplied from ASTM-cardes with blue color .The analysis of two patterns indicated that the experimental data fitted by a moderate ratio with simulated XRD such that the red circle refer to ABX_3 type structure (where A=Ni atom , B = Ti atom and X= Oxygen) .

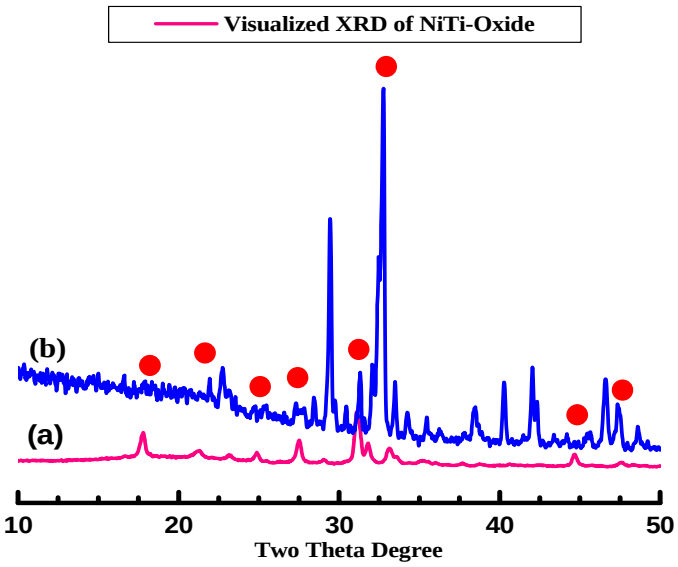

Fig.$1_{a,b}$ Theoretical and Experimental XRD-patterns of Ni-Ti-oxide with ABX_3 structure type.

The analysis of XRD-profile Fig.1_b confirmed that the ABX_3 structure is achieved with rhombohedral crystal lattice and R3-R(148) space group with lattice constant a = 5.47 and c = 55.12 Å .

A visualization study to the Ni-Ti-oxide with ABX_3 structure (where A=Ni atom , B = Ti atom and X= Oxygen) .was performed by using Diamond IMPACT CRYSTAL program to confirm the structure see Fig.(1c).

The study concerned by matching and comparison of lattice constants, torsion of bonding ,bond lengths and lattice volume .From Fig.1_c one can indicate that the Nickel ,Titanium-ionic radius are fitted and harmonized with the lattice volume and no torsions on the basic bonds of crystal structure of proposed Trigonal/Rhombohedral specially with present technique of preparation such that the angles found were 160 and 135 for Ti-O-Ti and Ni-O-Ni respectively.

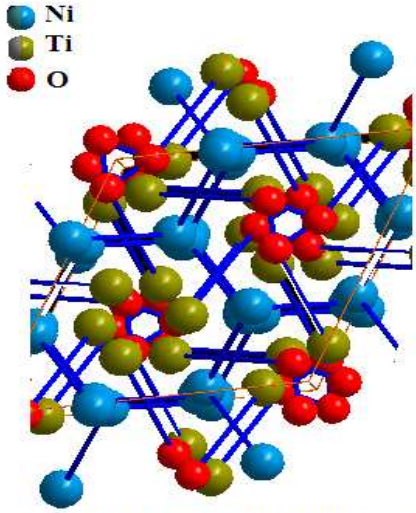

Fig.1c Visualized Trigonal/rhombohedral unit cell with 60 atoms .

The approximate ratios (area/area ratios) V_f of □-phase that represented in dark orange regions was found to be in between ~ 12-18 % of captured image area in the case of high solidification cooling rate (HSCR) .Furthermore the average grain size of Ni-super-alloy was estimated from Fig.2_b and ranged in between 2.3-5.4 µm which is fully consistent with those reported on literature [4,5].

Fig.2_b: shows high resolution three dimensional AFM-image recorded for Ni-super-alloy surface with HSCR applying tapping mode .For hyperfine 3D-structure of the surface , the experimental data supplied from AFM-device was forwarded to visualize the 3D-surface to be able to map the surface with maximum accuracy as possible see Figs.$2_{b,c}$.

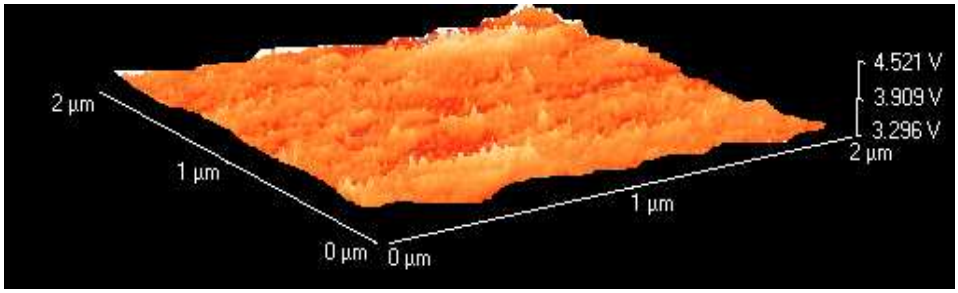

(Fig.2a) 3D-AFM tapping mode image of Ni-super-alloy .

Fig.2$_b$: displays 3D-mapping structure for very small area 0.35x0.35 µm of nickel-superalloy. It was noticeable that ~ 50 % of the surface morphology has z-axis (heights) ranged in between (0.26 – 6.5 µm represented by dark and pale blue) and only ~ 10 % has the heights higher than 6.5 µm . One can indicate that as strengthen phase ratio increases these heights will be increased and consequently increasing of □- phase will lead to corresponding increase in these heights .

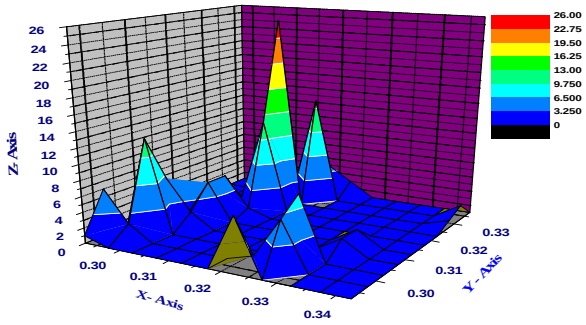

Fig.2$_b$: 3D-AFM-visualized image of Ni-super alloy.

This notification is confirmed as clear in Fig.2c such that the ratio of heights area dark zones to the homogeneous Ni-surface blue coloration is nearly equal to ~ 10-12 % which is identical to the estimated ratio of σ, and □-phases as confirmed from SE-micro-structural investigations with EDX-analyses see Table.2.

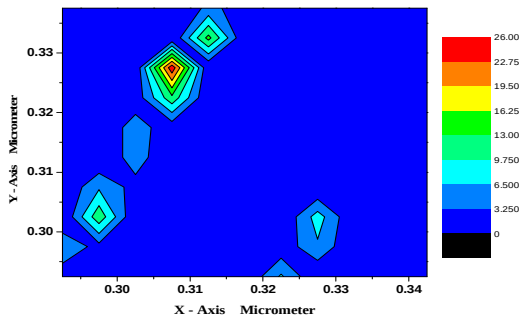

Fig.2$_c$: 2-D-vertical view image to map heights ratio of Ni-alloy .

EDX analysis was used to investigate the micro-segregation of the as cast specimens as shown in Table.2.

Table 2. EDX-elemental analysis of the micro-constituents in as cast alloys :

Elements / Phase	C	Cr	Mo	W	Ti	Co	Ta	Ni
η in as cast fine	0.19	4.31	0.84	1.17	15.94	7.19	3.00	Bal.
η in as cast coarse	1.89	5.72	1.90	2.37	14.07	8.33	6.46	Bal.
σ in as cast fine	0.31	33.85	9.73	4.68	5.05	11.15	1.20	Bal.
σ in as cast coarse	0.78	36.75	20.37	10.01	2.29	9.68	3.45	Bal.
MC in as cast fine	6.84	0.35	1.63	7.63	23.35	0.17	56.99	Bal.
MC in as cast coarse	6.35	1.26	1.93	8.01	20.32	0.63	56.71	Bal.

The partitioning coefficient, k', was calculated to characterize the degree of micro-segregation between dendrite core and interdendritic areas represented by eutectic γ/γ'. k' is the ratio between the element composition in dendrite core and the composition of the same element in eutectic γ/γ' zone. Table 2 shows the partition coefficient of important elements in the experimental Ni base superalloys used in this study. There are two groups of alloying elements according to the portioning coefficient. The first group of elements symbolized (G1) has k' higher than one such as W, Mo, Co and Cr. These elements segregate to the dendrite core during solidification.

However, the other group of elements symbolized as (G2) has k' lower than one like Al, Ti and Ta. These elements of this group are preferably segregated to the liquid during solidification process ultimately solidifying in interdendritic zones.

III.III.Laser Raman Spectroscopy:

Fig.3_a shows the laser raman spectra recorded for non-smothed casted Ni-alloy inside the range 300-550 cm^{-1} to identify different vibrational modes of nickel as major constituent of Ni-alloy . It was observed that the most common vibrating modes of Ni-O lie at 364 , 400 and 510 cm^{-1} by additional to vibrating mode appears at 476 cm^{-1} which is revealed to Ni_3O_4-phase . These results are in full agreement with those reported by [18].Furthermore there are some extra bands appear in Fig.3a like those lie at 309 ,379 ,446 ,461 and 519 cm-1 which are assigned as α- or β-Ni-OH vibrating modes as reported in [26] .

To identify some of minor phases constituent in the interfacial layers of Ni-base super-alloy another scanning of raman spectra was constructed in the range in between 800-1200 cm^{-1} as clear in Fig.3_b .

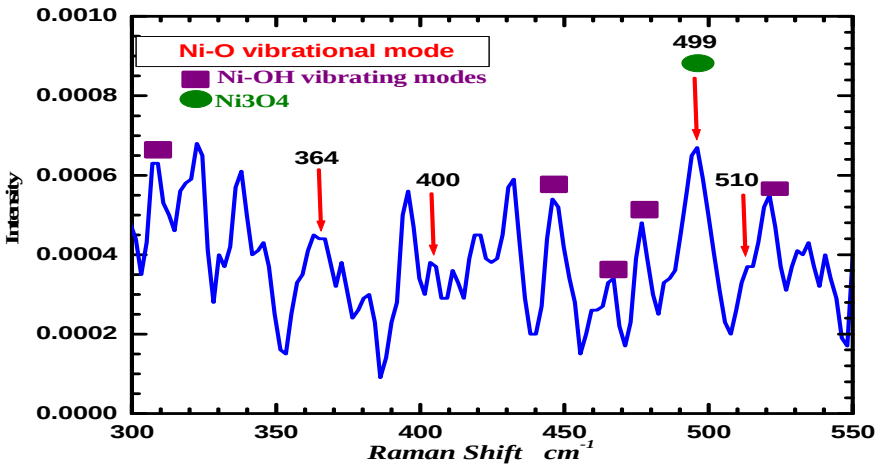

Fig.3a: Raman spectra recorded for casted –non-smoothed Ni-superalloy showing different vibrational modes of Ni-O moiety

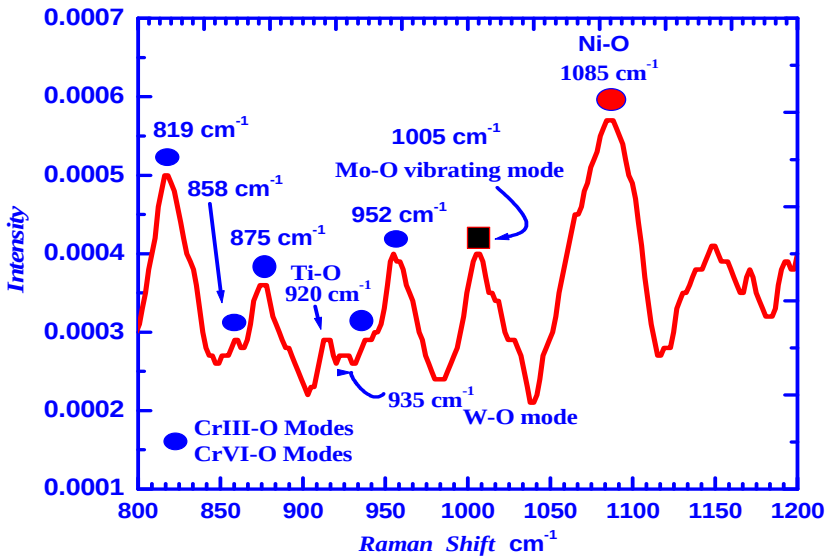

Fig.3$_b$: Raman spectra recorded for casted –non-smoothed Ni-superalloy showing different vibrational modes of Cr-O ,Ti-O and Mo-O moieties

It was obviously that there are multi-mixed vibrational modes assigned as the following sequence ;

(i) blue circles assignment which lie at 819 ,858,875, 940 and 952 cm^{-1}are attributable to CrIII-CrVI-O vibrational modes .

(ii) vibrational mode lies at 451,701 and 920 cm^{-1} is corresponding to Ti-O mode as confirmed by Ramya et al. [26] .

(iii) vibrational mode lie at 667,716 ,751 ,765 and 935 cm^{-1} is corresponding to W-O modes.
(iv) vibrational mode lies at 1005 cm^{-1} is corresponding to Mo-O vibrating mode and finally
(v) vibrational mode lie at 364,499,510, 1085 cm^{-1} which are belonging to Ni-O modes.

These results are consistent with those reported by [18,19,20 and 21] who investigated nickel-stainless alloy namely 316LN SS alloy by laser raman spectroscopy and they characterized different vibrating modes existed in the corroded interfacial surface of Ni-alloy .

The present results can be understood on the basis that Ni-based alloy could be passivated and form some metal-oxides according to the composition of the interfacial layers which means that Ni-based-alloy vibrating modes are preparative conditions dependent .

In the case of compounds of chromium on the passivated surface of Ni-alloy, they will exist as Cr(III) or Cr(VI). The moderate intensity peak at 860 cm^{-1} was attributed to Cr(III) and Cr(VI) mixed phase [27 - 32], which was slightly red shifted by a few wave numbers (around 871–885 cm^{-1}). Also, a weak peak around 520–570 cm^{-1} was due to Cr_2O_3 [29], which was diminished and overlapped with the frequencies of nickel oxides, thus indicating the possibility of existing in the form of $NiCr_2O_4$.

Apart from the presence of chromium and Titanium oxides, one could expect contributions of Ni as NiO at the surface layer. The reported value for the heat of formation of NiO was found to be equal −243.19 kJ mol^{-1} [33]. Cr_2O_3 has more negative heat of formation, i.e., −1058.58 kJ mol^{-1}. Hence, Cr would preferentially get oxidized and nickel was expected to be segregated at the oxide interface [34]. Garke et al. [35] showed that there was only a small amount of nickel in the oxide/metal interface, where there was no change in the nickel concentration and the nickel was in elemental state in the segregated zone. Since LRS cannot trace out individual elements [36], the presence of elemental Ni could not be detected. Even if all the Ti,W and Cr get oxidized, paving way to nickel oxidation, still it was difficult to sense the presence of traces of elemental-nickel due to the limited sensitivity of LRS.

CONCLUSIONS

The conclusive remarks inside this article could be briefed in the following points ;
1- The structural investigations confirmed that $NiTiO_3$ crystallized in rhombohedral structure with R3R space group and $NiTiO_3$ could be present on Ni-superalloy surface .
2- Laser Raman spectroscopy (LRS) could be used as qualitative technique to identify different phases constituents that present in the interfacial layer of the Ni-alloy surface since
a- Ni-O vibrational modes lie at 364,499,510, 1085 cm^{-1} .
b- vibrational mode lies at 1005 cm^{-1} is corresponding to Mo-O vibrating mode .
c- vibrational modes lie at 451,701 and 920 cm^{-1} are corresponding to Ti-O modes .
d- vibrational mode lies at819 ,858,875, 940 and 952 $cm^{-1}$are attributable to CrIII-CrVI-O vibrational modes .
e- vibrational mode lie at 667,716 ,751 ,765 and 935 cm^{-1} is corresponding to W-O modes .

REFERENCES

[1] O.H. Kriege and J.M. Baris, *Trans. ASM* **62 (1969)**, p. 195.
[2] R.E. Beddoe, P. Haasen and G. Kostorz In: P. Haasen, V. Gerold, R. Wagner and M.F. Ashby, Editors, *Decomposition of Alloys: The Early Stages*, Pergamon Press, Oxford **(1984).**
[3] K. Trinckauf, J. Pesicka, C. Schlesier and E. Nembach, *Phys. Stat. Sol. (a)* **131 (1992)**, p. 345.
[4] S.Q. Xiao and P. Haasen, *Acta Metall. Mater.* **39 (1991)**, p. 651.
[5] P. Staron and R. Kampmann, *Acta Mater.* **48 (2000)**, p. 713.
[6] S. Duval, S. Chambreland, P. Caron and D. Blavette, *Acta Metall. Mater.* **42 (1994)**, p. 185
[7] H.I. Aaronson and F.K. LeGoues, *Metall. Trans. A* **23 (1992 1915)**.
[8] A. Dupasquier, G. Kögel and A. Somoza, *Acta Mater.* **52 (2004)**, pp. 4707–4726.
[9] P. Gopalan, R. Rajaraman, B. Viswanathan, K.P. Gopinathan and S. Venkadesan, *J. Nucl. Mater.* **256 (1998),** p. 229.
[10] C.E. Macchi, A. Somoza, G. Santos, M. Petkov and K.G. Lynn, *Phys. Stat. Sol. (c)* **4 (2007),** p. 3542 and references therein.
[11] A.G. Khachaturyan, T.F. Lindsey and J.W. Morris Jr., *Metall. Trans. A* **19 (1988)**, p. 249.
[12] W.A. Soffa and D.E. Laughlin, *Acta Metall.* **37 (1989)**, p. 3019.
[13] W. R. Sun, J.H. Lee, S.M. Seo, S.J. Choe, Z.Q. Hu, *Mater. Sci. Technol*. 15**(1999)**p.1221.
[14] B.G. Choi, I.S. Kim, D.H. Kim, C.Y. Jo, *Mater. Sci. Eng.* A, 478**(2008)**p. 329.
[15] S.M. Seo, I.S. Kim, J.H. Lee, C.Y. Jo, H. Miyahara and K. Ogi, *Metall. Mater. Trans* A, 38**(2007)**p. 883.
[16] J. Gui and T.M. Devine, *Corrosion Science* 32 **(1991)**, p. 1105.
[17] D.S. Dunn, M.B. Bogart, C.S. Brossiaand and G.A. Cragnolino, *Corrosion* 56 **(2000)**, p. 470.
[18] D.L.A. de Faria, S. Venâncio Silva and M.T. de Oliveira, *Journal of Raman Specroscopy* 28 **(1997),** p. 873.
[19] K.N. Jallad and D. Ben-Amotz, *Material Science and Technology* 17 **(2001),** p. 479.
[20] R. Balasubramaniam, A.V. Ramesh Kumar and P. Dillmann, *Current Science* 85 **(2003),** p. 1546.
[21] F. Dubois, C. Mendibide, T. Pagnier, F. Perrard and C. Duret, *Corrosion Science* 50 **(2008)**, p. 3401.
[22] T. Kamimura and M. Stratmann, *Corrosion Science* 43 **(2001)**, p. 429.
[23] D. Cook, *Corrosion Science* 47 **(2005)**, p. 2550.
[24] D. Neff, L. Bellot-Gurlet, P. Dillmann, S. Reguer and L. Legrand, *Journal of Raman Specroscopy* 37 **(2006),** p. 1228.
[25] M. Yamashita, H. Miyuki, Y. Matsuda, H. Nagano and T. Misawa, *Corrosion Science* 36 **(1994),** p. 284.
[26] S. Ramya, T. Anita , H. Shaikh and R.K. Dayal ,*Corrosion Science* , 52, 6, **(2010)** p.2114-2121 .
[27] J.D. Ramsey and Richard L. McCreery, *Corrosion Science* 46 (2004), p. 1729
[28] T.L. Sudhesh, L. Wijesinghe and D.J. Blackwood, *Applied Surface Science* 253 **(2006)**, p. 1006.
[29] S. Kikuchi, K. Kawauchi, M. Kurosawa, H. Honjho and T. Yahishita, *Analytical Sciences* 21 **(2005)**, p. 197.

[30] J.D. Ramsey and R.L. McCreery, *Journal of the Electrochemical Society* 146 **(1999)**, p. 4076.
[31] J. Zhao, L. Xia, A. Sehgal, D. Lu, R.L. McCreery and G.S. Frankel, *Surface and Coatings Technology* 140 **(2001)**, p. 51.
[32] J.E. Maslar, W.S. Hurst, W.J. Bowers, J.H. Hendricks, M.I. Aquino and I. Levin, *Applied Surface Science* 180 **(2001)**, p. 102
[33] In: R.C. Weast, Editor, *Handbook of Chemistry and Physics* (65th ed.), CRC Press, Boca Raton, FL **(1984)**.
[34] X. Tian, Ricky K.Y. Fu, Lianwei Wang and Paul K. Chu, *Materials Science and Engineering* **A316 (2001)**, p. 200.
[35] B. Garke, C. Edelmann, R. Gunzel and J. Brutscher, *Surface Coating Technology* **93 (1997)**, p. 318.
[36] N.B. Colthup, L.H. Daly and S.E. Wiberley, Introduction to Infrared and Raman Spectroscopy (third ed.), Academic Press, New York **(1990).**